Integration of Structural Uncertainty and Robust Control

Clark Briggs[1]
ATA Engineering, San Diego, CA, 92128

Daniel C. Kammer[2]
University of Wisconsin, Madison, Wisconsin, 53706

Andrew White[3] and David Schwartz[4]
ATA Engineering, San Diego, CA, 92128

Designers using modern robust control methods can take advantage of uncertainty information about their plant. This may be as general as a frequency-based weighting function or it may be more specific information about the range of modal frequencies. Significant progress has been made in non-deterministic methods for predicting the uncertainty in structural design performance based on information about component properties. Working together, structures and controls can produce higher-performance controlled structural systems than they can separately. This synergy is demonstrated in this paper through the development of distribution statistics of the frequency response function for a structural system with uncertainty, with illustration of the improved controller performance that is possible with this information. This improved performance is a critical capability for many new systems that cannot be assembled and tested during development, such as large space telescopes and interferometers.

Nomenclature

C_r	=	covariance matrix
d_r	=	rth normalized design variable
FRF	=	frequency response function
FRF_{nom}	=	frequency response function of the nominal system
$\overline{FRF}$	=	frequency response function of the ensemble mean FRF
h	=	frequency response matrix
h'	=	perturbed modal frequency response matrix
$H(\omega)$	=	frequency response function
$\Im$	=	imaginary part of a complex value
$K, \widehat{K}, \widehat{K}'$	=	structural stiffness matrix for the nominal model, the modal model, and the perturbed model
$M, \widehat{M}, \widehat{M}'$	=	structural mass matrix for the nominal model, the modal model, and the perturbed model
R_r	=	correlation matrix
$\Re$	=	real part of a complex value
S_r	=	relation matrix
Δx	=	change in quantity x
z	=	nominal modal impedance matrix
z'	=	perturbed modal impedance matrix
$\bar{z}_r$	=	modal impedance sensitivity matrix for rth parameter
z	=	a complex random variable
z_r	=	the real part of a complex random variable

[1] Technical Director, Robotics and Control, and Associate Fellow.
[2] Professor, Dept of Nuclear Eng & Eng Physics, and Associate Fellow.
[3] Senior Project Engineer 1, Robotics and Control.
[4] Project Engineer 2, Robotics and Control.

z_i = the imaginary part of a complex random variable
ω_i = diagonal matrix of nominal system natural frequencies
ς_i = diagonal matrix of nominal system modal damping coefficients
σ_z = the covariance of a complex random variable
$\Phi, \hat{\Phi}$ = eigenvectors of the nominal and reduced model in physical coordinates
Ψ = eigenvectors of the reduced model in modal coordinates
ω_i = natural frequencies of the perturbed modal model
λ_i = eigenvalues of the perturbed modal model

I. Introduction

Many high-performance system designs depend critically on accurate knowledge of the system. Good modeling can support design well during the early part of a project, but component and system testing is almost always required prior to operational deployment. Traditional standard practice is to perform verification or proof tests of representative test articles. Component tests are performed to verify critical technical aspects; a variety of system tests are performed, for example, to validate the structural dynamics model or to proof test for launch loads.

For high-performance Aerospace systems, however, test articles and tests are extremely expensive and time consuming. As a result, repeated tests to characterize the uncertainty in key parameters are prohibitive at any level above component testing. Furthermore, system-level tests that can be used to characterize the as-deployed operational conditions simply cannot be constructed; gravity effects alter the structural response in ways that cannot be sufficiently accounted for, and thermal effects on structural and optical performance cannot be accounted for when the system cannot be tested in the available thermal-vacuum chamber.

New methods for uncertainty quantification have been developed to assist in support of design approval in the face of the missing tests. The goal is to provide quantifiable statements about the bounds on certain system properties based on an accumulation of lower-level tests and analyses. These component properties are propagated to system properties that can be used to describe the variability of system performance.

High-performance space systems utilize control systems for their stabilization, pointing and, often, autonomous operation. Designing the control system to be robust to uncertainties in the environmental loading has been a challenge largely met by stochastic control techniques. Modern robust control was developed to meet subsequent challenges presented by uncertain system properties. These robust controllers can guarantee stable, but suboptimal, control over a specified range of plant properties. Removing the conservatism in their performance depends critically upon better knowledge of the plant uncertainties.

We present in the following a cross-disciplinary example of designing robust controllers for plants with significant structural dynamics. The methods used in both structures and controls are representative but not complex. The intent is to show the benefits that derive from shared understanding between the two disciplines. Structural uncertainty propagation methods are used to model the variability in the structural frequency response function (FRF) between a controller's inputs and outputs. An upper and lower bound of the FRF are used as input to a robust control design process, and the controller's performance for nominal, off-nominal, and out-of-band structures is illustrated. The primary focus is on the nature of the handoff between structural modeling and control design.

II. Predicting Variability in Structural System Performance

A variety of methods have been developed to propagate component uncertainty to system-level uncertainty descriptions. Processes that utilize mixes of analytical and experimental methods are available. To have confidence in analytical predictions, the effects of uncertainty on system response must be well understood. Quantification of model uncertainty in structural dynamics and its propagation through large numerical simulations has been the focus of many investigations; there are too many studies to cite them all, but Refs. 1–4 represent a few of the more pertinent works. While an engineer may design a single structure based on the information given to them, the reality is that the item that is actually produced is just one in an ensemble of possible structures due to variations and uncertainties in geometry, material parameters, construction, etc. The result is a random population of systems, each with its own frequencies and mode shapes.

A large number of researchers have investigated the effects of structural uncertainty on system response. For example, Mace and Shorter[5] and Hinke, et al.[6] use linear perturbation methods to relate physical parameter uncertainties to uncertainty in modal parameters. The corresponding uncertainty in frequency response is then computed and the statistics determined through a Monte Carlo analysis. Hasselman and Chrostowski[7] combine linear perturbation methods with a covariance propagation approach to propagate modeling uncertainty into frequency response. This method avoids a Monte Carlo analysis; however, it only produces the variance in the

system response. In their applications, they also found that covariance propagation becomes less reliable in the vicinity of system resonances and anti-resonances. Small resonant frequency shifts due to modeling uncertainties cause corresponding shifts in the peaks of the frequency response. In the case of isolated frequencies, small changes in frequencies produce large changes in frequency response. Therefore, the linear perturbation results that covariance propagation is based upon tend to break down.

Kammer and Krattiger[8] expanded on the work done by Hasselman and Chrostowski[7] by developing a systematic approach for propagating uncertainty using covariance propagation in substructured models. The uncertainty in the substructure is not restricted to any specific type, such as the typical parameter uncertainty. It can be as general as uncertainty in the frequency response as determined by a series of substructure vibration tests. The approach is efficient; however, it is still inaccurate in predicting frequency response variance at resonances. This is due to the extreme nonlinear relation between uncertainty in frequency response and uncertainty in impedance at resonance. Kammer and Bonney[9] improved upon the linear perturbation prediction for frequency response and its second-order statistics in the vicinity of resonances by using a series expansion. The approach is summarized in Section IV.

The methods used here are representative. Our intention is to illustrate the benefits of cross fertilization between structures and controls.

III. A Simple Example

A simple spring mass system will be used to demonstrate the approach. The details of the model are in Ref. 16. A schematic of the system is shown in Fig. 1, but the image might be misleading in several respects. The masses are all nearly the same, despite the depiction of masses 1 and 6 as being larger. Also, there are slight differences in the individual masses and springs; these differences were imposed to obtain an irregular modal structure. Finally, the masses are all constrained to move in the vertical direction only; as a result, there is no rocking motion for the larger blocks of the diagram.

The nominal system is as shown, and variations considered only alter the spring values. The nominal positions are never altered. The nominal mode shapes are shown in Fig. 2, although the still images can make the motion difficult to visualize. The nominal system acceleration transfer function between excitation at mass 1 and acceleration response at mass 1 is shown in Fig. 3. Most of the results utilize this collocated point, although responses at other masses are shown on occasion.

The system is varied by considering changes to the spring values. Typically 4% variation is used, with 10% variation on occasion. A modal damping of 5% is usually assumed. Because the focus is foremost on the process, the bounds of the approximations are not greatly explored in this paper, but certain limitations that are apparent are pointed out on occasion.

These variations are considered as unknown properties that are each independent and modeled as Gaussian random variables. In more representative system models, these properties will certainly be of many different types and the estimates of their variability will come from a variety of sources, including component tests.

While there are many high-quality methods for determining the distribution of properties and for propagating these uncertainties to the system, our interest is more in using the uncertain system properties in downstream design processes. In the current case, we explore their use in the design of a structural motion control system.

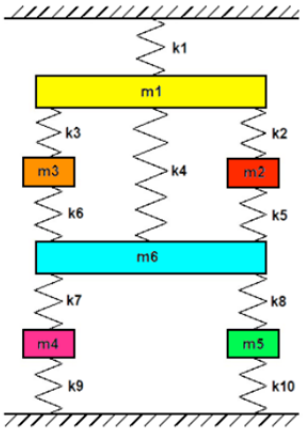

Figure 1. A simple structural example system.

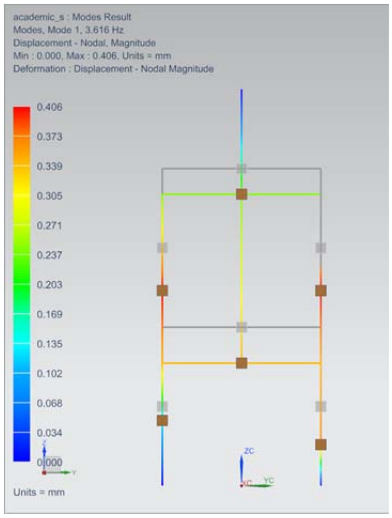

3.62 Hz

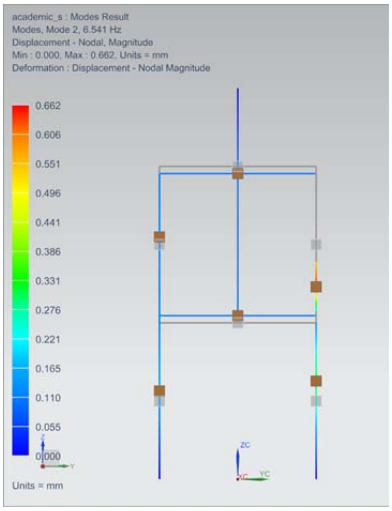

6.54 Hz

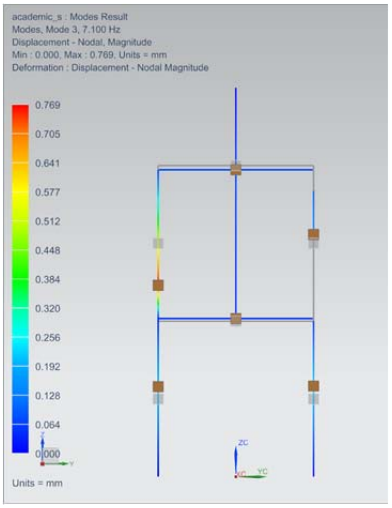

7.10 Hz

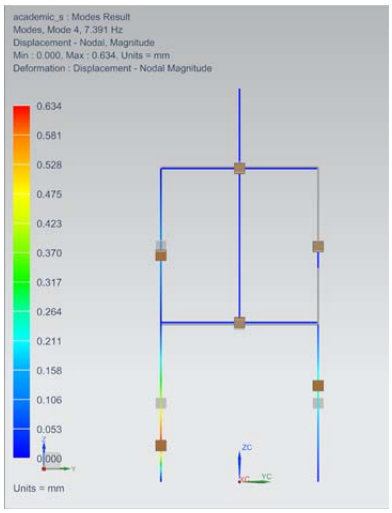

7.39 Hz

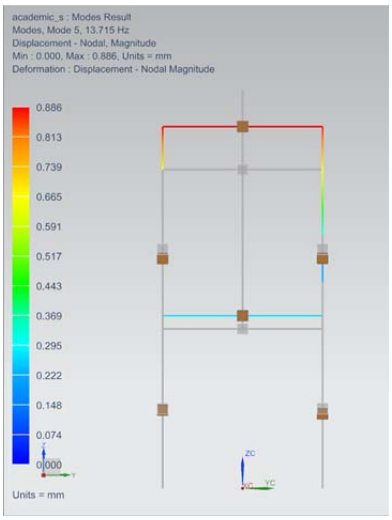

13.72 Hz

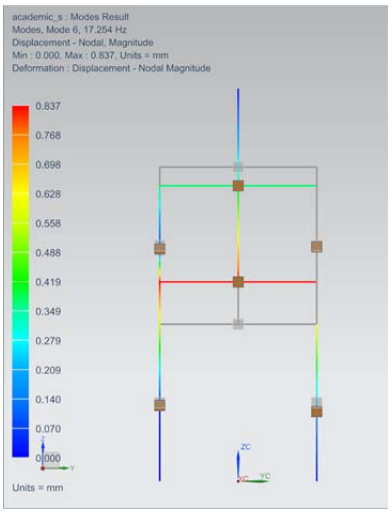

17.25 Hz

Figure 2. System modes for the simple example.

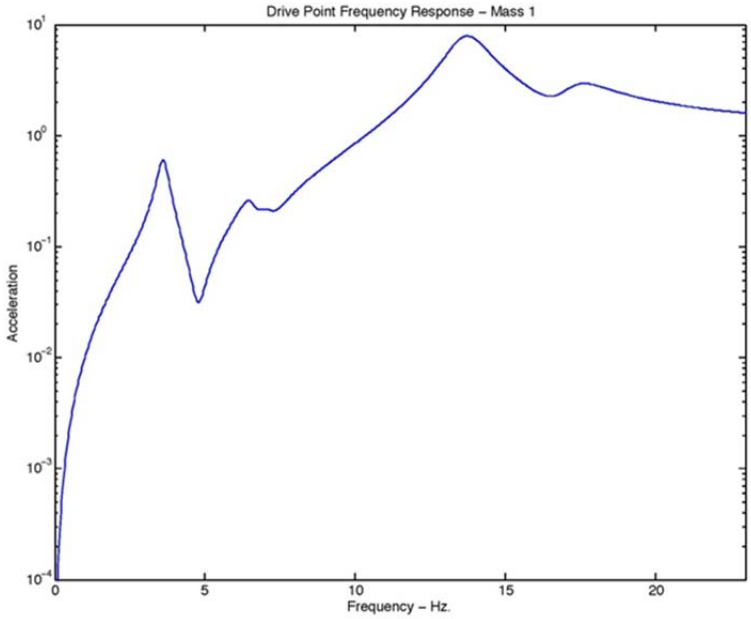

Figure 3. Nominal system FRF.

IV. Structural Uncertainty

The system FRF is a challenging system metric in part because the relationship between the linear system characterization as stiffness and masses requires an eigensolution to obtain the modes and an inversion to get the FRF from the modes. The two methods considered here differ in how the uncertainties are propagated from the modes to the FRF. The system eigenproblem and the linear sensitivities are obtained via Nastran Solution 200.

A. Structural Uncertainty Using Covariance Propagation

We first show the use of the method by Kammer and Bonney.[9] Covariance propagation is often used to propagate uncertainty and compute second-order response statistics. However, linear covariance propagation applied to frequency response is inaccurate at resonances due to nonlinearity.

The development of Ref. 9 is summarized here to illustrate the series expansion used in evaluating the frequency response matrix h and the numerical issues arising near resonances with low damping. The exposition begins with the nominal system modes and the linear sensitivities from a Nastran Solution 200 in hand. The method is amenable to an efficient implementation, although this has not been aggressively pursued at this point.

To maintain accuracy, reduce numerical instability, and reduce the size of the computational problem, uncertainty propagation is performed in the modal space of the nominal finite element model. A sufficient number of system modes are computed to accurately represent the dynamics within the desired frequency band. This is usually 1.5 to 2.0 times the highest frequency of interest. It is assumed that the nominal mode set is rich enough to span the uncertain system within the frequency range considered. In the case of parameter uncertainty, the modal impedance matrix at the frequency ω can be expanded in a first-order Taylor series about its nominal value in terms of the normalized design variables d_r using

$$z' = z + \sum_{r=1}^{n_p} \bar{z}_r \, \Delta d_r \tag{1}$$

The nominal modal impedance matrix is given by

$$z = -\omega^2 I + j\omega_i \varsigma_i + {\omega_i}^2 \tag{2}$$

Let h be the nominal system modal displacement frequency response matrix at frequency ω, then $h = z^{-1}$ or

$$hz = I \tag{3}$$

Assuming modal damping, the modal frequency response matrix is diagonal with the *i*th term given by

$$h_{ii} = (\omega_i^2 - \omega^2 + j2\varsigma_i\omega_i)^{-1} \tag{4}$$

corresponding to the *i*th nominal system mode. If the nominal system is perturbed, Eq. (3) becomes

$$h'z' = (h + \Delta h)(z + \Delta z) = I \tag{5}$$

which can be expanded and rearranged to give

$$\Delta h = -h'\Delta z h \tag{6}$$

This is the exact expression for the uncertainty, or change, in the frequency response for a given change, or uncertainty, in the impedance. Unfortunately, the corresponding perturbed modal frequency response h' is not known. The usual covariance propagation approach is based on the first-order approximation of Eq. (6) given by

$$\Delta h = -h\Delta z h \tag{7}$$

This approximation is accurate for small values of system uncertainty at frequencies that are removed from the resonances. As a resonance is approached, the relationship between the change in modal frequency response and the change in modal impedance becomes very nonlinear, and the linear approximation in Eq. (7) becomes poor.

As an alternative, Eq. (5) can be arranged to give the exact expression for uncertainty in frequency response in the form

$$\Delta h = -h\Delta z h(I + \Delta z h)^{-1} \tag{8}$$

The matrix inverse in Eq. (8) can be expanded in an infinite series to give

$$\Delta h = -h\Delta z h(I + \Delta z h + \cdots + (-1)^{k-1}(\Delta z h)^{k-1} + \cdots) \tag{9}$$

If the spectral radius of matrix $\Delta z h$ is less than 1.0, or, equivalently, if all the eigenvalues are within the unit circle, the infinite series in Eq. (9) can be approximated by a finite number of terms. For example, in the case of uncertainty due to stiffness alone, the expression in Eq. (9) will converge for the *i*th isolated mode if the fractional uncertainty in the *i*th modal frequency due to the change in stiffness is less than the corresponding modal damping coefficient

$$\frac{\Delta\omega_i}{\omega_i} < \varsigma_i \tag{10}$$

In general, it has been found that for a fixed level of uncertainty, as the damping level is reduced, more terms are required in Eq. (9) as a resonance is approached.

Defining the matrix

$$\Delta_k = (\Delta z h)^{k-1}\Delta z \qquad k = 1, \infty \tag{11}$$

the *r*th-order approximation can be rewritten as

$$\Delta h_r = h(\textstyle\sum_{k=1}^{r}(-1)^k\Delta_k)h \tag{12}$$

Note that $r = 1$ corresponds to the first-order or linear approximation used in straightforward covariance propagation. In terms of modal coordinates, the nominal physical frequency response matrix at frequency ω is given by

$$H = \Phi_s h \Phi_a^T \tag{13}$$

in which Φ_s is the modal matrix row partitioned to the sensor locations and Φ_a is the modal matrix row partitioned to the input locations. The *r*th approximation for the uncertainty in the physical frequency response matrix is then given by

$$\Delta H_r = \Phi_s h(\sum_{k=1}^{r}(-1)^k \Delta_k) h \Phi_a^T \tag{14}$$

Uncertainty in velocity or acceleration response can be determined by multiplying Eq. (14) by $i\omega_i$ and $-{\omega_i}^2$, respectively. The matrix ΔH_r in Eq. (14) can be stacked columnwise to form the vector, p_r. Outer products of the vector with itself can be formed and expectations can be taken to give the associated covariance matrix

$$C_r = R_r - \bar{p}_r \bar{p}_r{}^* \tag{15}$$

in which * represents a complex conjugate transpose, $R_r = \overline{p_r p_r{}^*}$ is the correlation matrix, and the overbar represents the expectation operator. An analogous procedure can be used to derive the associated relation matrix

$$S_r = \overline{(p_r - \bar{p}_r)(p_r - \bar{p}_r)^T} \tag{16}$$

The covariance and relation matrices provide complete information regarding the second-order statistics of the frequency response. Details of the derivations can be found in Ref. 1.

B. Structural Uncertainty Using Monte Carlo and a Reduced Model

An alternative method that produces very similar results is described briefly in this section. Our intent is to show a degree of independence of the method for determining the FRF uncertainty while focusing on the nature of the handoff to the subsequent control design. Again, beginning with the nominal system modes and the linear sensitivities from a Nastran Solution 200, the machinery of Attune™ is used to construct a Monte Carlo ensemble of FRFs. Attune is a program for test/analysis correlation and model updating and uses IMAT for the underlying structural data formats and methods.[10,15] It has methods for computing a variety of structural response metrics, such as the FRF, from perturbed models. Both Attune and IMAT work in MATLAB, so computing FRF statistics and plotting results is straightforward. The methods used by Attune are very efficient since design sensitivity coefficients can be calculated at a small fraction (10% to 20%) of the cost of standard normal modes analysis.

In anticipation of supporting large system finite element models, a model reduction is performed based on a modal analysis—although for the small example problem, all six modes are kept. The resulting mass and stiffness are

$$\widehat{M} = \Phi^T M \Phi, \widehat{K} = \Phi^T K \Phi \tag{17}$$

The reduced mass matrix is a diagonal matrix of modal masses, and the reduced stiffness matrix is a diagonal matrix of modal stiffnesses. The modal stiffness sensitivity ΔK and the modal mass sensitivity ΔM from the Nastran Solution 200 are multiplied by the Monte Carlo sample draws and summed with the nominal modal matrices to form the perturbed system matrices $\widehat{M}'$ and $\widehat{K}'$. The perturbed modes and frequencies are then computed from the eigenproblem:

$$\left(\widehat{K}' - \lambda_i \widehat{M}'\right)\psi_i = 0, \widehat{\Phi} = \Phi\Psi, f_i = \frac{\sqrt{\lambda_i}}{2\pi} \tag{18}$$

where $\widehat{\Phi}$ are the eigenvectors of the reduced model in physical coordinates and Ψ are the eigenvectors of the reduced model in modal coordinates. This eigenproblem is the size of the number of modes in the reduced model, and this is significantly smaller than the original large system model.

The FRF for this ensemble member is

$$H(\omega) = \sum \frac{(\widehat{\Phi}\Psi)^T \Psi \widehat{\Phi}}{\sqrt{({\omega^2}_i - \omega^2)^2 + (2\zeta\omega\omega_i)^2}} \tag{19}$$

where ${\omega^2}_i = \lambda_i$ are the perturbed natural frequencies, and the elements of $\widehat{\Phi}$ in the numerator represent the input and response physical coordinates. The summation is over the modes of the reduced and perturbed model.

Figure 4 shows an ensemble acceleration FRF for 10% stiffness uncertainty and 5% modal damping.

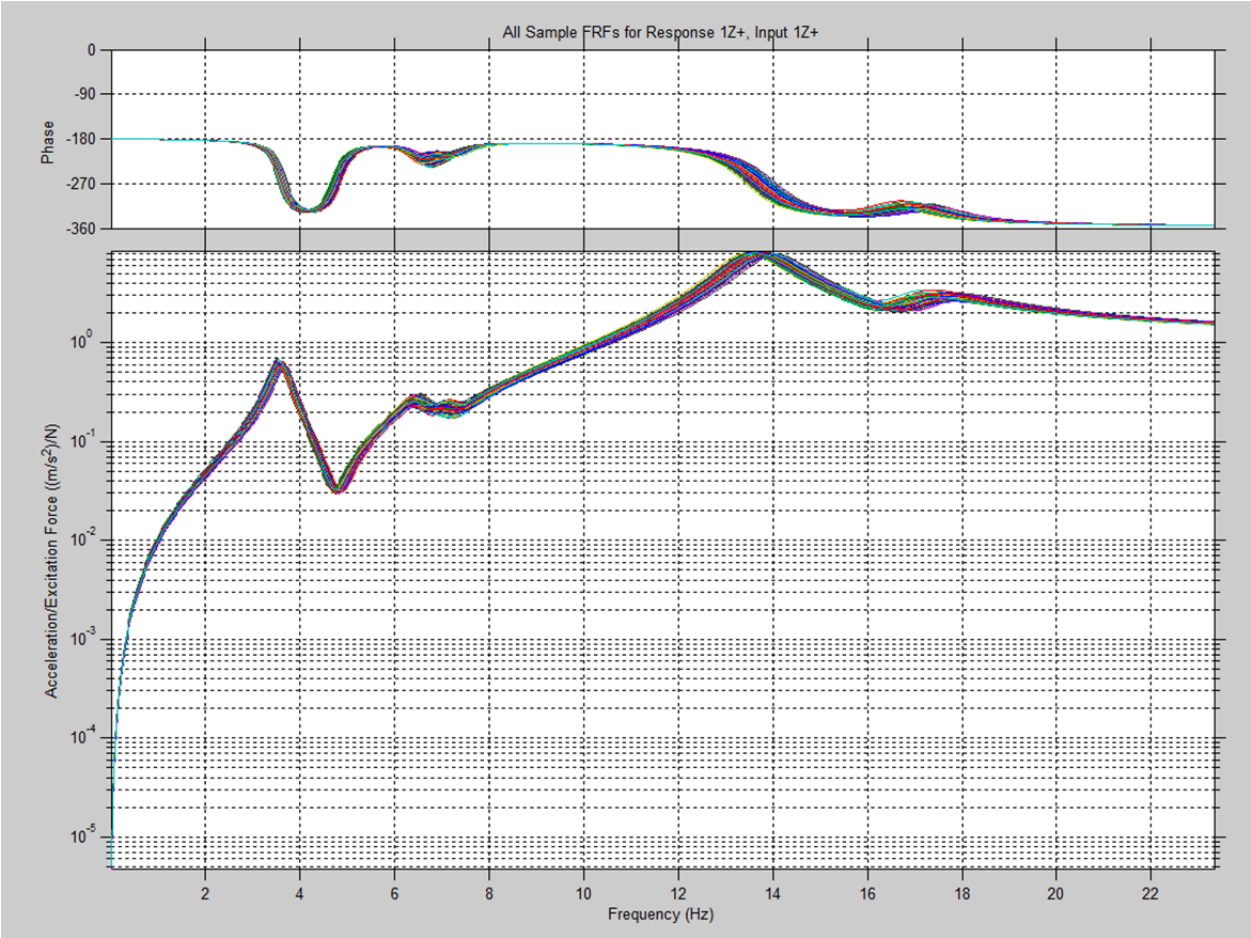

Figure 4. FRF ensemble.

C. Toward Understanding FRF Uncertainty

Recent developments in communication signal processing have firmly established the basis for extending stochastic real processes to stochastic complex-valued processes.[11–13] For example, Ref. 14 puts estimators such as widely linear maximum likelihood estimation on firm ground. To our knowledge, the development of FRFs has not been extended in this way, even though the FRF plays a prominent role in electronic system analysis. Our goal is to provide the same sound basis for building, understanding, and using such constructs as "the ± 2σ FRF." This is the expression that captures structural uncertainty, to be used for designing controllers that are robust to uncertain structural dynamics.

Analysis of complex-valued functions begins with casting the complex random variable z (here, our FRF) as the sum of two real random variables.

$$z = x + iy \tag{20}$$

This approach can be accepted even though we start with real random variables in our structural description. This is not at all to be based on the potentially wide variety of uncertain parameters and their possible distributions, but rather on the several nonlinear operations present in the computation of the FRF. Whether the uncertain parameters are independent or correlated, or are Gaussian distributions or otherwise, as long as the operations are linear, the influence of each can be discerned. The real and complex parts of the FRF develop in complicated ways first through the modal eigenvalue solution and then through the inverse to the FRF. In addition, we commonly assume modal damping, which is directly implemented in the imaginary term of the modal response. Thus, we can fully expect the real and imaginary parts of the FRF to be modeled as correlated random variables of unknown (and surely not Gaussian) distribution.

With care, then, it is now straightforward to develop the second-order statistics of this random variable. From Ref. 7, the covariance is based on the squared magnitude

$$\sigma_z^2 = E\left[\left(z - E(z)\right)\left(z - E(z)\right)^*\right], \tag{21}$$

whereas the pseudo-covariance is based on the square

$$\tilde{\sigma}_z^2 = E\left[\left(z - E(z)\right)^2\right]. \tag{22}$$

As noted in Ref. 14, terminology varies widely; the pseudo-covariance is sometimes called the complementary variance or the relation function.

Related terms must also be discussed—in particular, the covariance of the real part and covariance of the imaginary part. Reference 14 shows that

$$\sigma_{z_r}^2 = \frac{1}{2}\left(\sigma_z^2 + \Re(\tilde{\sigma}_z^2)\right) \tag{23}$$

$$\sigma_{z_i}^2 = \frac{1}{2}\left(\sigma_z^2 - \Re(\tilde{\sigma}_z^2)\right) \tag{24}$$

$$cov(z_r, z_i) = \frac{1}{2}\left(\Im(\tilde{\sigma}_z^2)\right) \tag{25}$$

The correlation coefficient ρ is

$$\rho = \frac{cov(z_r, z_i)}{\sqrt{\sigma_{z_r}^2 \sigma_{z_i}^2}} \tag{26}$$

The FRF is a complex-valued function of frequency ω. That is, at each spectral line, the FRF is a complex number with real and imaginary parts. If an ensemble of FRF samples is prepared, say, by Monte Carlo sampling of the uncertain structural parameters and computing the FRF, at some frequency ω the complex numbers would form a cloud. The nominal system FRF could be one such point in the cloud. The mean and covariance of the real parts and the imaginary parts can be used to construct contours of equal probability. Two examples are shown in Fig. 5.

As we have noted, the FRF distributions are not expected to be Gaussian normal because of the nonlinear inverse from the modal description to the FRF. The two plots in Fig. 5 show examples of this. The ovals are the 95th percentile of the sample, and the oblateness of the oval is a reflection of the correlation coefficient ρ. Higher-order statistical moments could be used to capture the FRF distributions more accurately, but, since our interest here is in illustrating the process and developing a shared vocabulary, this is not pursued further at this time.

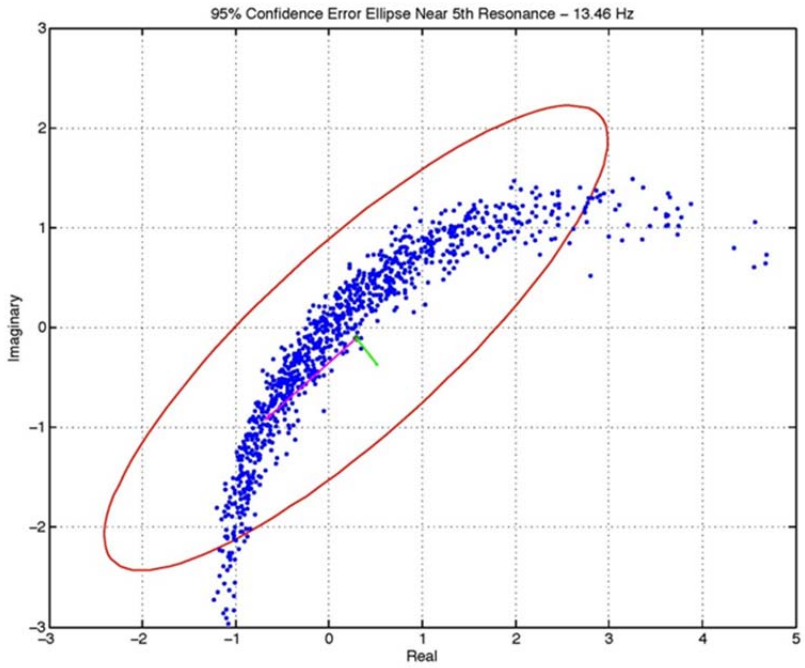

a. Near a resonance

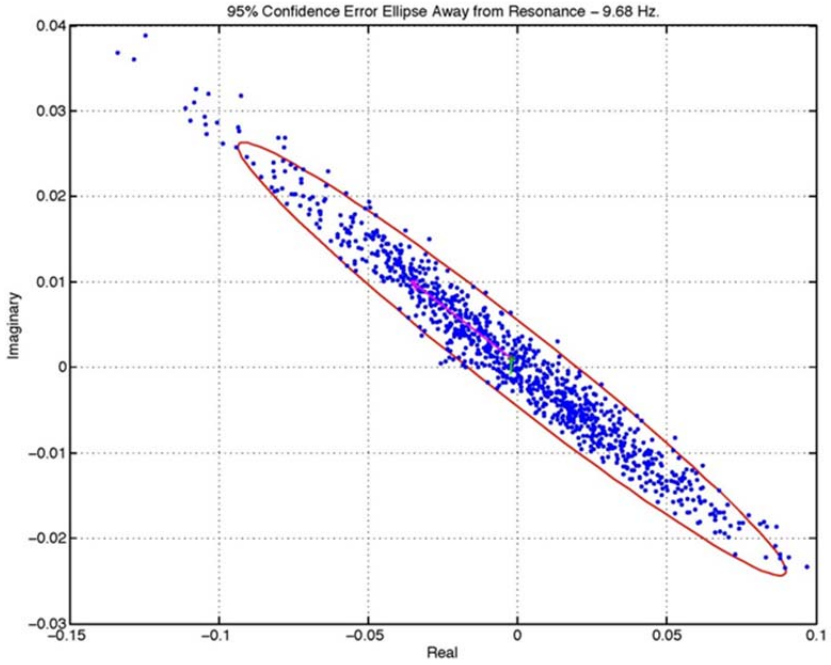

b. Away from a resonance

Figure 5. Example FRF point clouds in the complex plane.

The Nyquist plot is commonly used in control design and shows the complex FRF in the imaginary plane as a function of frequency. In robust control, the plant uncertainty is traditionally shown as magnitude-bounded zones overlaid with the nominal FRF. For our uncertain spring and mass model, this diagram is as shown in Fig. 6.

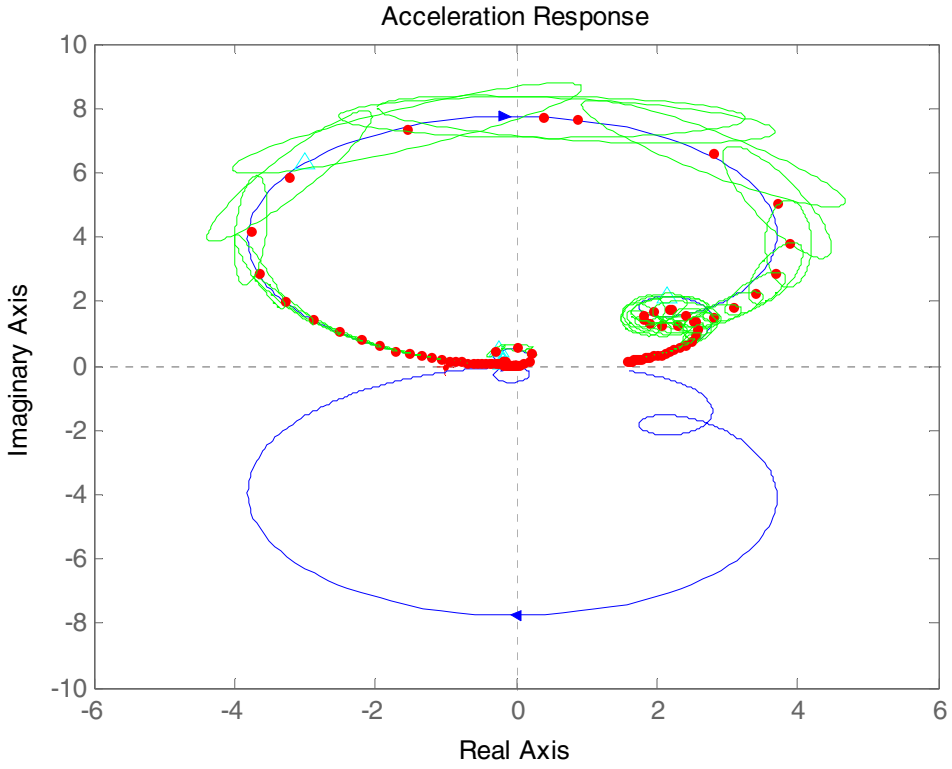

Figure 6. Nominal structural FRF with 2σ uncertainty bounds.

Stability margins are derived from the minimum distance between −1+0i and any uncertainty boundary. Here, this is a lightly damped structural system FRF which is clearly stable. The margins are then available for exploitation by the robust controller.

The desired handoff to controls design is a description of the degree of variability in the system FRF. At this point, we have a description based on the statistics of the real part and the imaginary part individually, as in Fig. 7a and Fig. 7b. The FRF variability can also be cast as the statistics of the magnitude and the phase individually; see Fig. 7c and Fig. 7d.

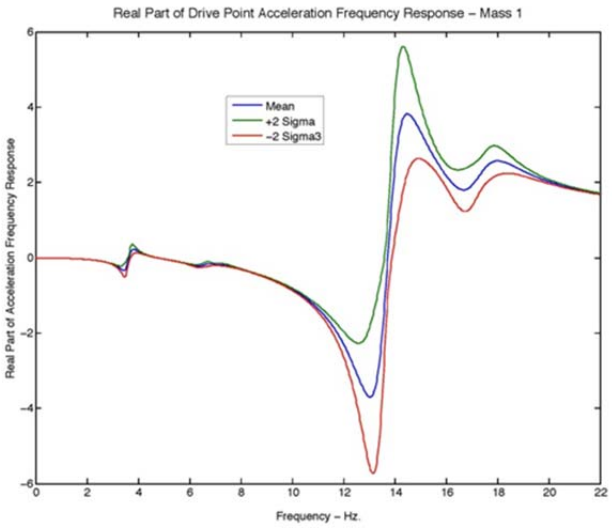

a. Acceleration response real part

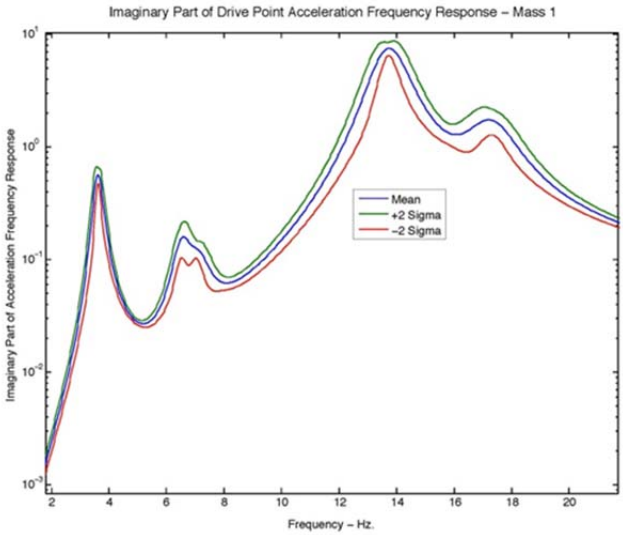

b. Acceleration response imaginary part

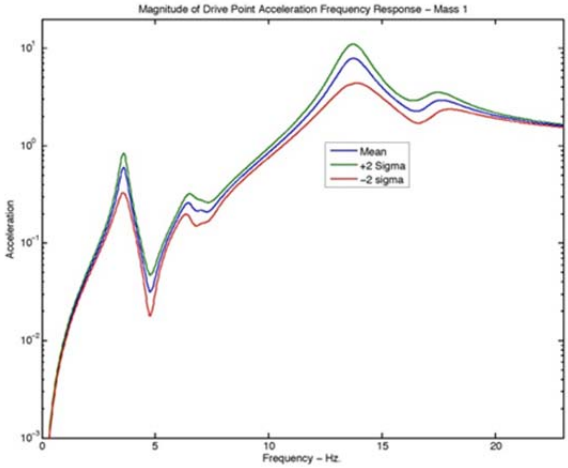

c. Acceleration response magnitude

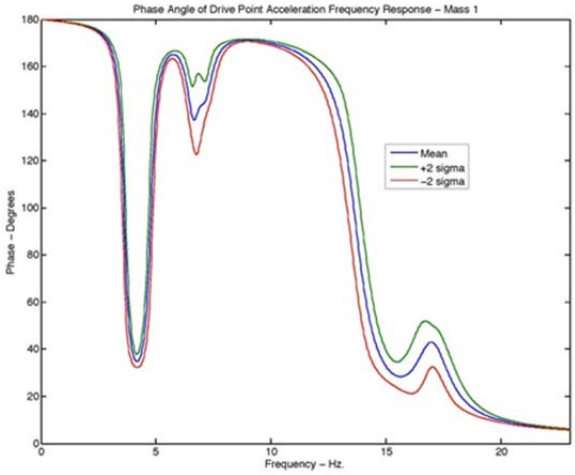

d. Acceleration response phase

Figure 7. FRF real and imaginary parts.

If the bounding 2σ ovals in Fig. 6 are plotted densely, the eye sees outer and inner bounds that are readily interpreted as the FRF magnitude 2σ bounds. A good approximation to the bounding hull is simply the oval points that are the maximum and minimum distance from the origin. These system upper and lower bounds are shown in Fig. 8.

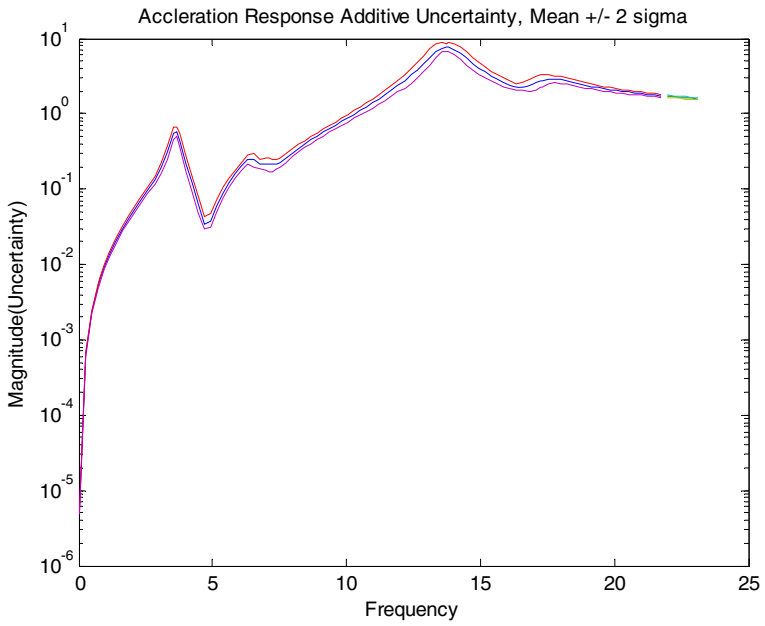

Figure 8. System FRF bounds based on 2σ maximum and minimum distance points.

The FRF formulations shown in Fig. 7 and Fig. 8 are intended to be the interface in the handoff to controller design. The project team would decide how much variability is to be used as the basis for the controller design as expressed in the number of standard deviations chosen for upper and lower uncertainty bounds. This establishes the portion of the possible structural systems that will be within the robust bounds of the controller and what the probability will be of encountering a system outside the controller's design bounds.

In the next section, we illustrate robust controller design and provide examples of controller performance when posed against potential systems instances.

V. Application to Robust Control

We imagine controllers for systems where structural dynamics form a dominant characteristic of the plant. The foregoing FRF descriptions are intended to inform the control design with a new form of knowledge about the specific variability of the plant as well as its origins. In the following, we illustrate the vulnerability of a naïve controller designed for good performance against the nominal plant by posing it against off-nominal instances. We then move on to briefly show modern robust control design methods that can take as input limited expressions of the uncertainty in the plant. We will show the improved performance that robust controllers can achieve when posed with instances within the design envelope, as well as when posed with plant instances that constitute extreme draws from the population outside the design envelope. Our goal is to establish the design trade for the project team of good enough performance against likely instances versus costly performance against rare instances.

Perturbations are commonly expressed as either additive or multiplicative. For additive uncertainties,

$$G = G_o(s) + \Delta(s) \tag{29}$$

For multiplicative uncertainties,

$$G = [I + \Delta(s)]G_o(s) \tag{30}$$

See Fig. 9 for a block diagram expression of these models. We seek relevant expressions for Δ(s) in terms of the FRF. Current working examples are shown in Fig. 10.

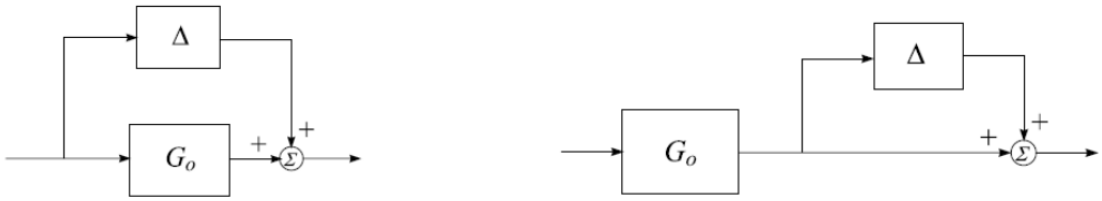

a. Additive uncertainty b. Multiplicative uncertainty

Figure 9. System architectures with plant uncertainty.

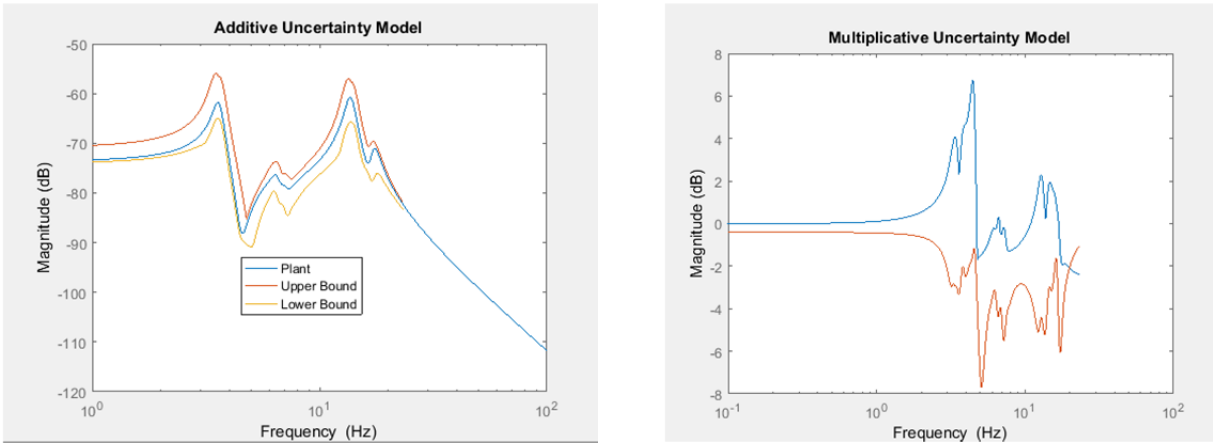

a. Additive uncertainty b. Multiplicative uncertainty

Figure 10. Structural FRF examples of additive and multiplicative uncertainties.

To illustrate the value of robust controller design, consider the task of driving mass M1 at the top of the stack with collocated position measurement and a design goal of a step input response time. This naïve controller, which was designed simply without any information other than the nominal structure, is a fourth-order controller with four poles and four zeros. The controller was designed to have a rise time of 2 seconds. As shown by inspection of the Bode plot in Fig. 11, the resultant controller has an integration stage, a notch filter near the first plant resonance, and a derivative stage at high frequencies to increase the phase margin.

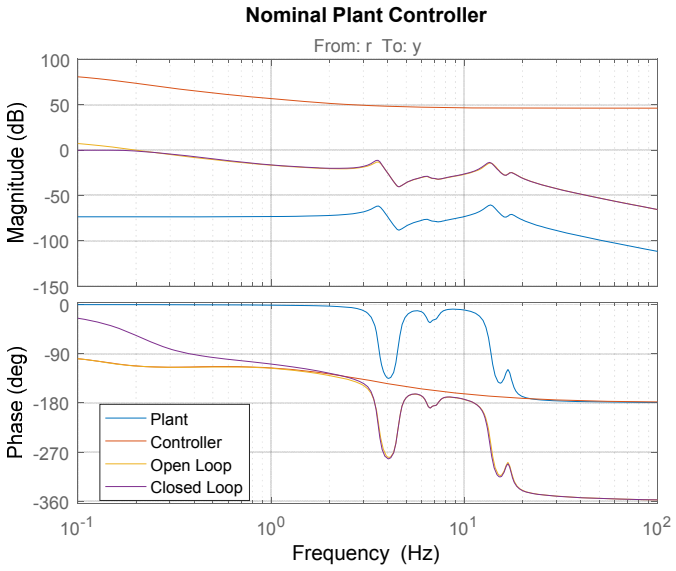

Figure 11. A simple controller for step response of mass 1.

Fig. 12 shows the controller posed against the nominal structure, achieving a maximum overshoot of 4%. When posed against some other variation of the structure, the overshoot is worse at 8%.

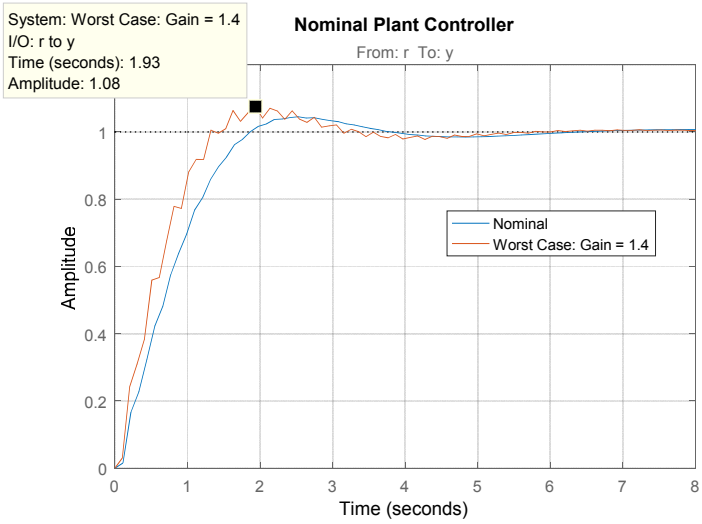

Figure 12. Controller performance against nominal and off-nominal structural plant.

To extend this controller design example, the robust control H_∞ algorithm was used to design a fourth-order controller with the goal of responding to a step command within 2 seconds and maintaining 9 dB gain and 66 degree phase margins using only the nominal plant. Figure 13 shows the controller architecture and the controller's step response with the nominal and off-nominal plants. The step response shows ~7% overshoot.

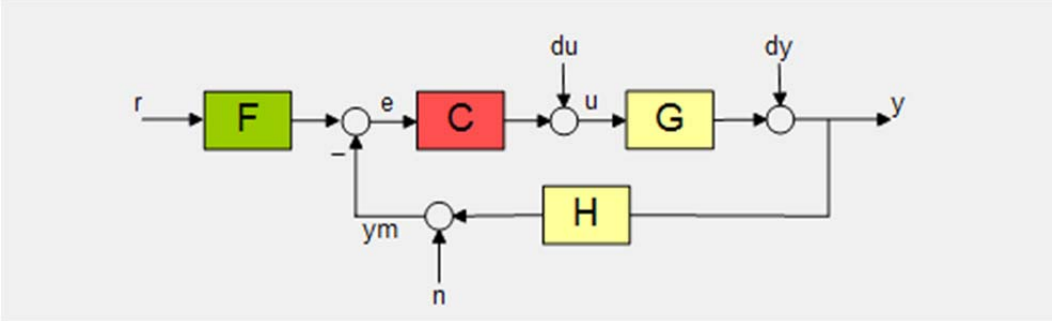

a. Robust controller architecture

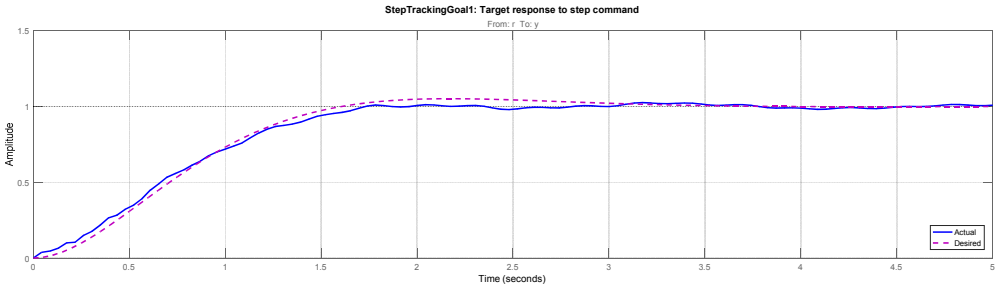

b. Controller response to a step command with the nominal plant

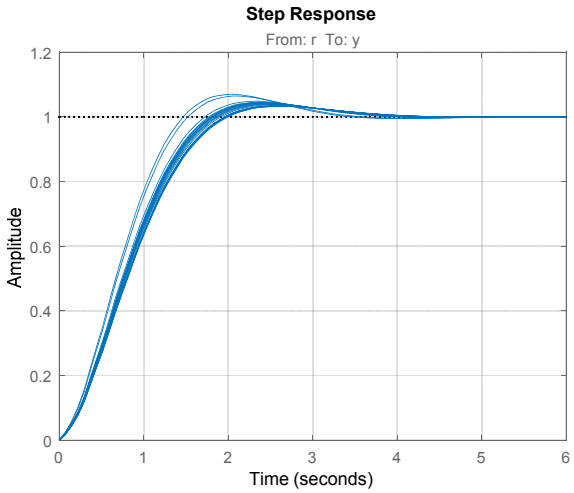

c. Controller response to off-nominal plants

Figure 13. Robust controller architecture and step response.

To include uncertainty, simple upper and lower bounds for an additive uncertainty were used (Fig. 14a), which would result in the bounded plant FRF shown in Fig. 14b.

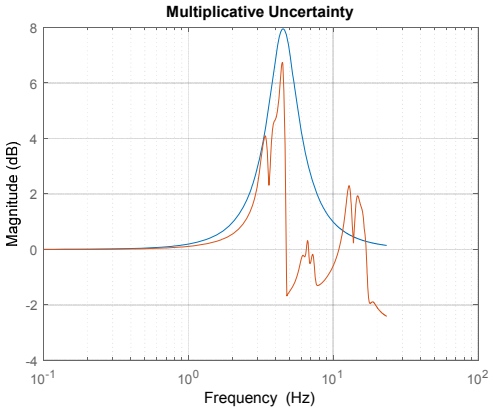

a. Example uncertainty bounds

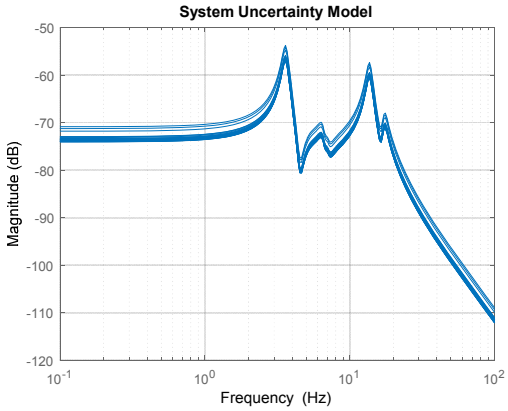

b. Uncertainty-bounded FRF

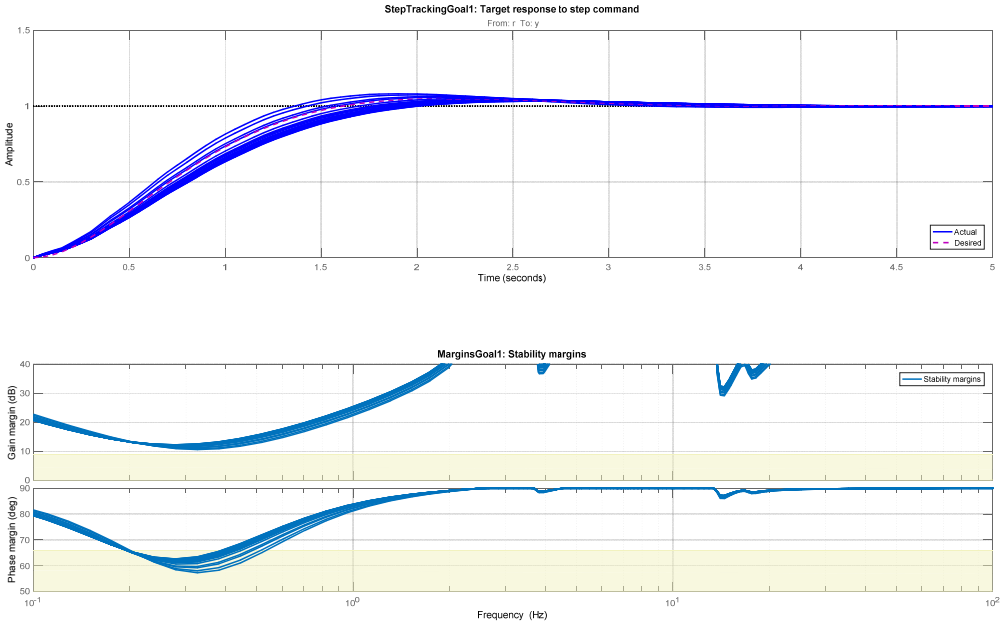

c. Robust controller performance and margins

Figure 14. Additive uncertainty for the spring mass example problem.

Tuning with the uncertain plant yields a more uniform step response with lower overshoot; see Fig. 14c. The algorithm meets the margin goals for most frequencies.

The controller can be posed against plants that are outside the 2σ bounds. The step response for such out-of-band samples is shown in Fig. 15. For one such sample, the naïve nominal plant controller is unstable. For an even worse sample, the robust controller is stable, at least, but shows poor performance. With the uncertainty quantification method developed here, these samples can be tied to the population statistics to identify a probability of occurrence.

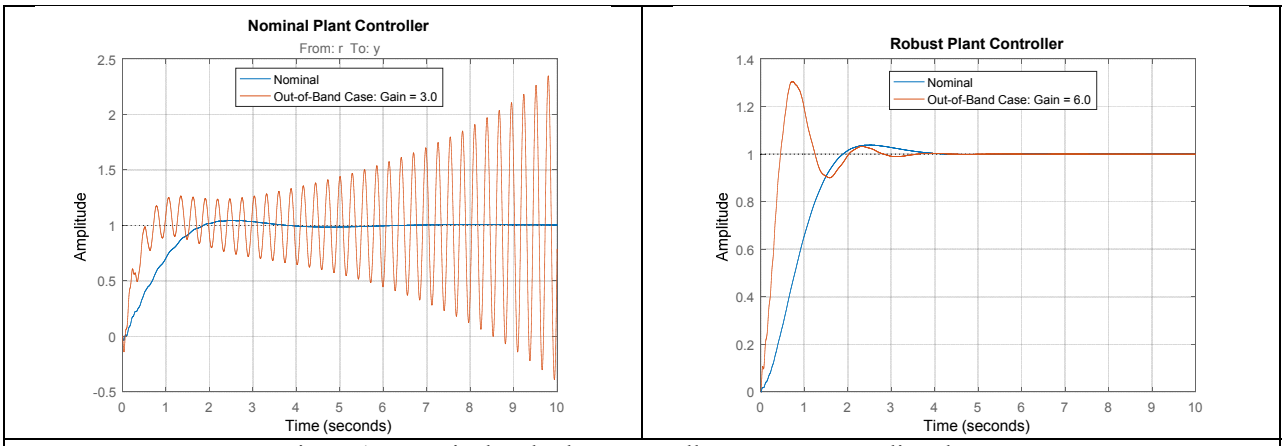

Figure 15. Nominal and robust controller response to outlier plants.

VI. Discussion and Conclusion

With this insight into structural uncertainty and its use in robust control design, the machinery is now in place to consider several system-level challenges. Here are a few scenarios.

Suppose the system engineers, using their system performance model, determine that the design does not turn and settle fast enough. The controls designer can point to the actuators as underpowered, which is a common reality, but now the designer can say that the gain cannot be turned up any higher because the mode at 3.5 Hz, say, has too much associated uncertainty. The sensitivity of that mode to uncertain structural parameters can be checked for those parameters with the largest impact on that mode. The structural team can then consider the causes and propose additional investments to improve knowledge. For example, there might be significant uncertainty in a hand-laid-up composite box, and the investment might be more automation to reduce the part-to-part variability. Or the structural team might say that the joint stiffness that was loosely modeled with added springs might be improved based on more detailed joint models.

This knowledge can be used in project risk assessment and mitigation. Suppose the robust control design was based on the 2σ bounds on the structural uncertainty. The robust design can ensure stability against plants within those bounds, but the performance of certain outliers might still be below desired levels. For much more extreme plant instances, the controller design might not be stable or the performance might be intolerably poor. Perhaps particular extreme plant instances can result in direct solar impact on the imager or the star tracker. The plant population statistics can be used to estimate the expected cost of off-nominal performance given utility and value functions. The project management can then make financial trades to invest more heavily in reducing the plant uncertainty, further tuning the control design, or even adding other system components to mitigate extremely poor performance. Examples of such additional investments might be new system autonomy to catch incipient catastrophic events or system identification during commissioning or even ongoing maintenance.

Further work, to be captured in a following paper, is being done to illustrate the process on a more representative structure such as an aircraft, providing a more typical modal structure and uncertainty bounds more aligned with our experiences. Future work might include testing using a representative scale aircraft structure and an embedded controller, funding permitting. These tests could include demonstration of control performance when the structure is modified.

References

[1]Rebba, R., S. Huang, Y. Liu, and S. Mahadevan. "Statistical Validation of Simulation Models." *International Journal of Materials and Product Technology* 25, No. 1 (2006): 164–181.

[2]Hemez, F.M., A.C. Rutherford, and R.D. Maupin. "Uncertainty Analysis of Test Data Shock Responses." 24th International Modal Analysis Conference. Saint Louis, MO, 2006.

[3]Basseville, M., and A. Benveniste. "Handling Uncertainties in Identification and Model Validation: A Statistical Approach." 24th International Modal Analysis Conference. Saint Louis, MO, 2006.

[4]Hasselman, T.K. "Quantification of Uncertainty in Structural Dynamic Models." *Journal of Aerospace Engineering* 14 (2001): 158–165.

[5]Mace, B.R., and P.J. Shorter. "A Local Modal/Perturbation for Estimating Frequency Response Statistics of Built-Up Structures with Uncertain Properties." *Journal of Sound and Vibration* 242 (2001): 793–811.

[6]Hinke, L., F. Dohnal, B.R. Mace, T.P. Waters, and N.S. Ferguson. "Component Mode Synthesis as a Framework for Uncertainty Analysis." *Journal of Sound and Vibration* 324 (2009): 161–178.

[7]Hasselman, T.K., and J.D. Chrostowski. "Propagation of Modeling Uncertainty Through Structural Dynamic Models." 35th AIAA Structures, Structural Dynamics, and Materials Conference. Hilton Head, SC, 1994. 72–83.

[8]Kammer, D.C., and D. Krattiger. "Propagation of Uncertainty in Substructured Spacecraft Using Frequency Response." *AIAA Journal* 51, No. 2 (2013: 353–361.

[9]Kammer, D.C., and M. Bonney. "Improved Estimation of Frequency Response Covariance." *AIAA Journal* 24, No. 11 (1986): 1872–3.

[10]Attune, automated test-analysis correlation and model updating software, Ver. 2.1.4, ATA Engineering, San Diego, CA, Apr 2016.

[11]Ollila, E., V. Koivunen, and H.V. Poor. "Complex-Valued Signal Processing – Essential Models, Tools and Statistics." *Proceedings of the Information Theory and Applications Workshop*, San Diego, CA, 2011. 1–10.

[12]Eriksson J., E. Ollila, and V. Koivunen. "Essential Statistics and Tools for Complex Random Variables." *IEEE Transactions on Signal Processing*. 58, No. 10, October 2010.

[13]Eriksson J., E. Ollila, and V. Koivunen. "Statistics for Complex Random Variables Revisited." *Proceedings of the 34th IEEE International Conference on Acoustics, Speech, and Signal Processing*, Taipei, Taiwan. 2009. 3565–3568.

[14]Trampitsch, S. "Complex-Valued Data Estimation, Second-Order Statistics and Widely Linear Estimators." Master's thesis, University of Klagenfurt. 2013.

[15]IMAT, a suite of utilities for sharing data between MATLAB, analysis tools, and test software, Ver. 6.1, ATA Engineering, San Diego, CA, Mar 2016.

[16]Kammer, D.C., and S. Nimityongskul. "Frequency Band Averaging of Spectral Densities for Updating Finite Element Models." *Journal of Vibration and Acoustics* 131, No. 4, 2009.